PROCEEDINGS OF SCIENCE

Search for the forbidden charm decays $D^0 \to h'h\ell'\ell$

Fergus WILSON[*†]
STFC Rutherford Appleton Laboratory, Harwell Campus, Didcot, Oxon, OX11 0QX, UK
E-mail: Fergus.Wilson@stfc.ac.uk

We report a search for nine lepton-number-violating (LNV) and three lepton-flavor-violating (LFV) neutral charm decays of the type $D^0 \to h'^- h^- \ell'^+ \ell^+$ and $D^0 \to h'^- h^+ \ell'^\pm \ell^\mp$, where h and h' represent a K or π meson and ℓ and ℓ' an electron or muon. The analysis is based on 468 fb^{-1} of e^+e^- annihilation data collected at or close to the $\Upsilon(4S)$ resonance with the *BABAR* detector at the SLAC National Accelerator Laboratory. No significant signal is observed, and we establish 90% confidence level (C.L.) upper limits on the branching fractions in the range $(1.0-30.6)\times 10^{-7}$. The limits are between one and three orders of magnitude more stringent than previous measurements.

European Physical Society Conference on High Energy Physics - EPS-HEP2019
10-17 July, 2019
Ghent, Belgium

[*]Speaker.
[†]on behalf of the *BABAR* Collaboration

PoS(EPS-HEP2019)270

Many models beyond the SM predict LFV or LNV, possibly at rates approaching those accessible with current data. LNV is a necessary condition for leptogenesis as an explanation of the baryon asymmetry of the Universe. If neutrinos are of Majorana type, the neutrino and antineutrino are the same particle and some LNV processes become possible.

We present a search for nine $D^0 \to h'^- h^- \ell'^+ \ell^+$ LNV decays and three $D^0 \to h'^- h^+ \ell'^\pm \ell^\mp$ LFV decays, with data recorded with the *BABAR* detector at the PEP-II asymmetric-energy e^+e^- collider operated at the SLAC National Accelerator Laboratory. The data sample corresponds to $424\,\text{fb}^{-1}$ of e^+e^- collisions collected at the center-of-mass (CM) energy of the $\Upsilon(4S)$ resonance (on peak) and an additional $44\,\text{fb}^{-1}$ of data collected 40 MeV below the $\Upsilon(4S)$ resonance (off peak) [1]. The branching fractions for signal modes with zero, one, or two kaons in the final state are measured relative to the normalization decays $D^0 \to \pi^-\pi^+\pi^+\pi^-$, $D^0 \to K^-\pi^+\pi^+\pi^-$, and $D^0 \to K^-K^+\pi^+\pi^-$, respectively. The D^0 mesons are identified from the decay $D^{*+} \to D^0\pi^+$ produced in $e^+e^- \to c\bar{c}$ events. The *BABAR* detector is described in detail in Ref. [2].

Candidate D^0 mesons are formed from four charged tracks. Particle identification (PID) is applied to the charged tracks and the same criteria are applied to the signal and normalization modes. The four tracks must form a good-quality vertex with a χ^2 probability for the vertex fit greater than 0.005. A bremsstrahlung energy recovery algorithm is applied to the electrons, in which the energy of photon showers that are within a small angle (typically 35 mrad) of the initial electron direction are added to the energy of the electron candidate.

The candidate D^{*+} is formed by combining the D^0 candidate with a charged pion with a momentum in the laboratory frame greater than $0.1\,\text{GeV}/c$. A vertex fit is performed with the D^0 mass constrained to its known value and the requirement that the D^0 meson and the pion originate from the interaction region. The χ^2 probability of the fit is required to be greater than 0.005. After the application of the D^{*+} vertex fit, the D^0 candidate momentum in the PEP-II center-of-mass system, p^*, is required to be greater than $2.4\,\text{GeV}/c$.

The normalization yields are extracted with a two-dimensional unbinned maximum-likelihood (ML) fit to the D^0 meson mass $m(D^0)$ and the mass difference, $\Delta m = m(D^{*+}) - m(D^0)$, between the reconstructed masses of the D^{*+} and D^0 candidates; the ranges are $1.81 < m(D^0) < 1.91\,\text{GeV}/c^2$ and $0.143 < \Delta m < 0.148\,\text{GeV}/c^2$. The normalization modes Δm and $m(D^0)$ distributions are each represented by multiple Cruijff [3] or Crystal Ball [4] functions with a shared mean. The backgrounds are represented by an ARGUS threshold function [5] for Δm and a Chebyshev polynomial for $m(D^0)$. All parameters, apart from the ARGUS threshold endpoint, are allowed to vary.

For the LFV and LNV signal decays, a multivariate discriminant using nine observables as input is applied to reduce the backgrounds from $e^+e^- \to c\bar{c}$. The observables are based on the kinematics of the final-state particles and the event shape. The D^0 meson mass $m(D^0)$ is required to be within three times the reconstructed $m(D^0)$ mass resolution, with the resolution depending on the number of $e^\pm$ in the decay. The signal yields are extracted with a one-dimensional unbinned ML fit to the range $0.141 < \Delta m < 0.201\,\text{GeV}/c^2$ for signal modes with two kaons and $0.141 < \Delta m < 0.149\,\text{GeV}/c^2$ for all other signal modes. The signal probability density function (PDF) is a Cruijff function with parameters obtained by fitting the signal MC. The background is modeled with an ARGUS function with an endpoint that is set to the same value that is used for the normalization modes. The signal PDF parameters and the ARGUS endpoint parameter are fixed in the fit. All other background parameters and the signal and background yields are allowed to vary.

The main sources of systematic uncertainty in the branching fraction determinations are associated with the model parameterizations used in the fits and the normalization procedure, signal MC modeling, fit bias, tracking and PID efficiencies, luminosity, backgrounds from intermediate decays to $e^+e^-\gamma$, and the normalization mode branching fraction. Some of the tracking and PID systematic effects cancel in the branching fraction determinations since they affect both the signal and normalization modes.

The fitted yields for the normalization modes $D^0 \to \pi^-\pi^+\pi^+\pi^-$, $D^0 \to K^-\pi^+\pi^+\pi^-$, and $D^0 \to K^-K^+\pi^+\pi^-$ are $28\,470 \pm 220$, $260\,870 \pm 520$, and 8480 ± 110, with reconstruction efficiencies $(24.7 \pm 0.2)\%$, $(20.1 \pm 0.2)\%$, and $(19.2 \pm 0.2)\%$, respectively. For the LFV and LNV signal modes, no significant signal is seen and 90% C.L. branching fraction upper limits between $(1.0 - 30.6) \times 10^{-7}$ are determined. These are between one and three orders of magnitude more stringent than previous results. The fits are shown in Fig. 1 and the results are given in Table 1.

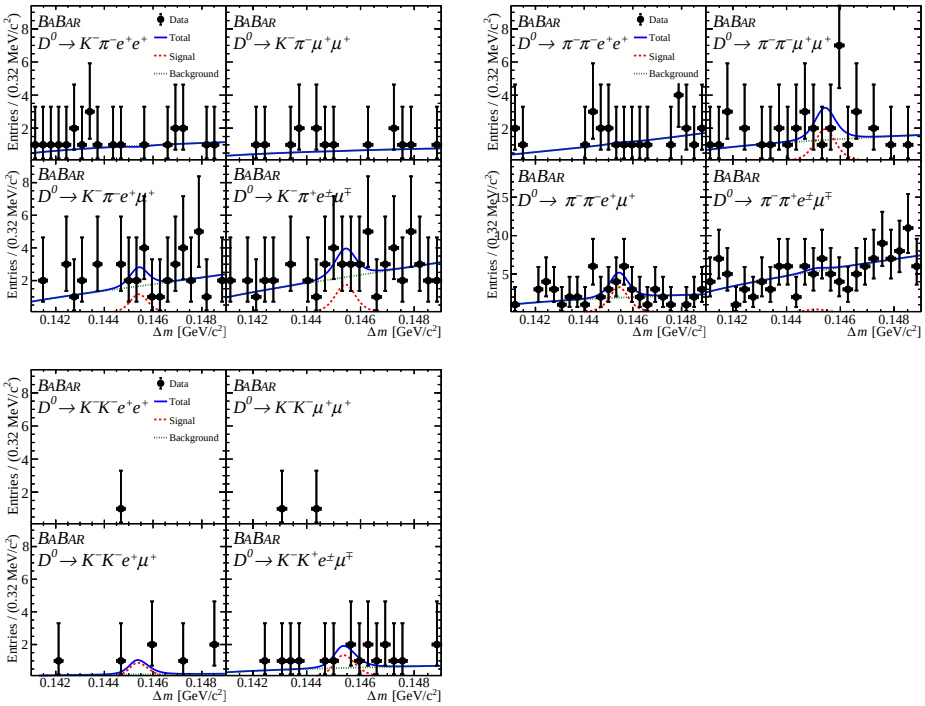

Figure 1: Fits to nine $D^0 \to h'^-h^-\ell'^+\ell^+$ LNV decays and three $D^0 \to h'^-h^+\ell'^\pm\ell^\mp$ LFV decays.

References

[1] J.P. Lees *et al.*, (*BABAR* Collaboration), Nucl. Instrum. Methods Phys. Res., Sect. A **726**, 203 (2013).

[2] B. Aubert *et al.*, (*BABAR* Collaboration), Nucl. Instrum. Methods Phys. Res., Sect. A **479**, 1 (2002); A **729** 615 (2013).

[3] The Cruijff function is a centered Gaussian with different left-right resolutions and non-Gaussian tails: $f(x) = \exp(-(x-m)^2/(2\sigma^2_{\mathrm{L,R}} + \alpha_{\mathrm{L,R}}(x-m)^2))$.

[4] T. Skwarnicki, Thesis, Institute of Nuclear Physics, Krakow, DESY-F31-86-02.

Table 1: Summary of fitted signal yields with statistical and systematic uncertainties, reconstruction efficiencies, branching fractions with statistical and systematic uncertainties, 90% C.L. branching fraction upper limits (U.L.), and the previous limits [9, 10].

Decay mode $D^0 \to$	$N_{\rm sig}$ (candidates)	$\varepsilon_{\rm sig}$ (%)	$\mathscr{B}$ ($\times 10^{-7}$)	$\mathscr{B}^{\rm U.L.}_{90\%}$ ($\times 10^{-7}$)	$\mathscr{B}^{\rm U.L.}_{90\%}$ [PDG] ($\times 10^{-7}$)
$\pi^-\pi^-e^+e^+$	$0.22 \pm 3.15 \pm 0.54$	4.38	$0.27 \pm 3.90 \pm 0.67$	9.1	1120
$\pi^-\pi^-\mu^+\mu^+$	$6.69 \pm 4.88 \pm 0.80$	4.91	$7.40 \pm 5.40 \pm 0.91$	15.2	290
$\pi^-\pi^-e^+\mu^+$	$12.42 \pm 5.30 \pm 1.45$	4.38	$15.41 \pm 6.59 \pm 1.85$	30.6	790
$\pi^-\pi^+e^\pm\mu^\mp$	$1.37 \pm 6.15 \pm 1.28$	4.79	$1.55 \pm 6.97 \pm 1.45$	17.1	150
$K^-\pi^-e^+e^+$	$-0.23 \pm 0.97 \pm 1.28$	3.19	$-0.38 \pm 1.60 \pm 2.11$	5.0	28 [10]
$K^-\pi^-\mu^+\mu^+$	$-0.03 \pm 2.10 \pm 0.40$	3.30	$-0.05 \pm 3.34 \pm 0.64$	5.3	3900
$K^-\pi^-e^+\mu^+$	$3.87 \pm 3.96 \pm 2.36$	3.48	$5.84 \pm 5.97 \pm 3.56$	21.0	2180
$K^-\pi^+e^\pm\mu^\mp$	$2.52 \pm 4.60 \pm 1.35$	3.65	$3.62 \pm 6.61 \pm 1.95$	19.0	5530
$K^-K^-e^+e^+$	$0.30 \pm 1.08 \pm 0.41$	3.25	$0.43 \pm 1.54 \pm 0.58$	3.4	1520
$K^-K^-\mu^+\mu^+$	$-1.09 \pm 1.29 \pm 0.42$	6.21	$-0.81 \pm 0.96 \pm 0.32$	1.0	940
$K^-K^-e^+\mu^+$	$1.93 \pm 1.92 \pm 0.83$	4.63	$1.93 \pm 1.93 \pm 0.84$	5.8	570
$K^-K^+e^\pm\mu^\mp$	$4.09 \pm 3.00 \pm 1.59$	4.83	$3.93 \pm 2.89 \pm 1.45$	10.0	1800

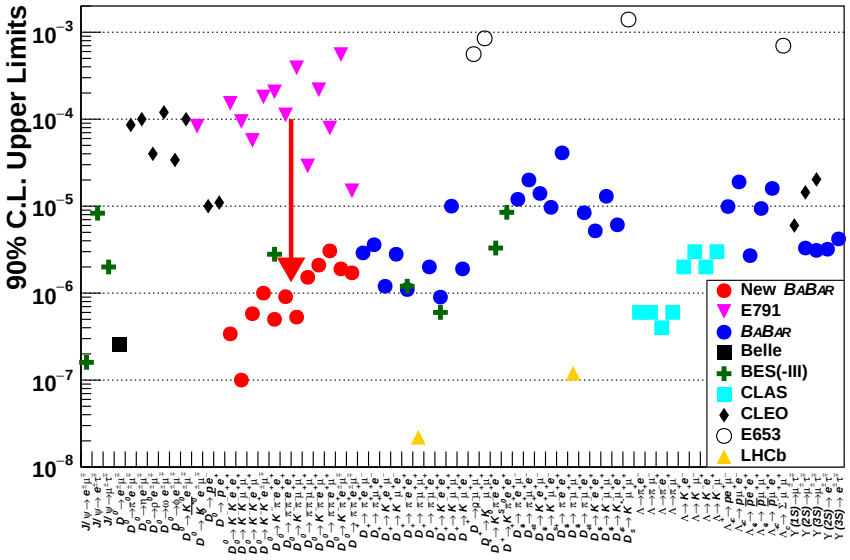

Figure 2: Summary of some 90% C.L. $\mathscr{B}$ upper limits from PDG and this analysis ("New *BABAR*").

[5] H. Albrecht *et al.*, (ARGUS Collaboration), Phys. Lett. B **241**, 278 (1990).

[6] R. Aaij *et al.*, (LHCb Collaboration), Phys. Lett. B **757**, 558 (2016).

[7] G. Feldman and R.D. Cousins, Phys. Rev. D **57**, 3873 (1998).

[8] M. Pivk and F.R. le Diberder, Nucl. Instrum. Methods Phys. Res., Sect. A **555**, 356 (2005).

[9] Particle Data Group, M. Tanabashi *et al.*, Phys. Rev. D **98**, 032001 (2018).

[10] M. Abkilim *et al.*, (BES-III Collaboration), Phys. Rev. D **99**, 112002 (2019).